Interfacial properties of poly(maleic acid-alt-1-alkene) disodium salts at water/hydrocarbon interfaces

Marcela D. Urzua [a], Fernando J. Mendizábal [a], Walton J. Cabrera [b], Hernán E. Ríos [a,*]

[a] *Departamento de Química, Facultad de Ciencias, Universidad de Chile, Casilla 653, Correo Central, Santiago, Chile*
[b] *Departamento de Química, Casilla 121, Universidad Arturo Prat, Iquique, Chile*

Abstract

The interfacial properties of poly(maleic acid-alt-1-alkene) disodium salts at hydrocarbon/water interfaces are determined. In all the studied systems, the interfacial tension decreases markedly with the polyelectrolyte concentration as the side-chain length increases. The results of the standard free energy of adsorption, ΔG^0_{ads}, are a linear function of the number of carbon atoms in the polyelectrolyte side chain. The contribution to ΔG^0_{ads} per mol of methylene group varies from -0.64 to -0.52 kJ/mol for the *n*-octane/water to *n*-dodecane/water interfaces. ΔG^0_{ads} data also reveal that the adsorption process is mainly determined by adsorption efficiency. Comparatively, the adsorption effectiveness seems to play a less important role. The theoretical interaction energies calculated for the insertion of one hydrocarbon molecule into the space formed by two neighboring polyelectrolyte side chains are in good agreement with the experimental results. The latter results are consistent with van der Waals-type interactions between the hydrocarbon molecules and the polyelectrolyte side chains.

Keywords: Amphipathic polyelectrolytes; Water–hydrocarbon interfaces; Adsorption free energies

1. Introduction

The interfacial properties of amphipathic polyelectrolytes are a relevant topic that has not been extensively studied, due probably to experimental complications in obtaining reliable and reproducible interfacial tension results in the high dilution range where interfacial phenomena are relevant.

In a previous paper the interfacial properties of poly (mono-*n*-alkylmaleic acid-alt-styrene) monosodium salts at the *n*-octane/water interface were studied [1]. These water-soluble polyelectrolytes show a less negative free energy of adsorption, ΔG^0_{ads}, as the side chain of the polyelectrolyte increases. A contribution of -2.55 kJ per mol of methylene groups was found for ΔG^0_{ads}, whereas the areas covered by the comonomeric unit at the interface increase as the polyelectrolyte side chain increases. Only the octyl derivative covers an at this interface area which is similar to that found in the same system but in the air/water surface [2], where covered areas do not depend on the side chain length. On the other hand, decyl and dodecyl polyelectrolytes at the *n*-octane/water interface cover areas greater than those of the octyl polymer, assuming more extended conformations at the interface. Comparing results at the air/water surface with those at the *n*-octane/water interface, the conclusion is that the octyl derivative extends its side chains vertically to the *n*-octane phase, probably due to the similarity between *n*-octane molecules and octyl lateral chains.

In recent work, the interfacial properties of bromide salts of poly(4-vinylpyridine) *N*-alkyl quaternized at the $CHCl_3$/water interface were studied [3]. The hexyl, octyl, and decyl polyelectrolytes were water-insoluble, but soluble in chloroform; therefore the polyelectrolyte adsorption process was studied from chloroform to the chloroform/water interface. The trend of the interfacial activity

* Corresponding author.
E-mail address: hrios@uchile.cl (H.E. Ríos).

suggests that this property is mainly determined by the hydrophilic/hydrophobic balance between the polar bromide pyridinium groups and the aliphatic apolar side chains. In fact, the hexyl derivative shows higher interfacial activity as compared with polyelectrolytes containing longer side aliphatic chains such as octyl and decyl. Consequently, the total free energy of the adsorption process was principally determined by the bromide pyridinium group contribution of −36 kJ/mol. Recently, Olea and co-workers [4] reported the interfacial properties of dipotassium salts of poly(maleic acid-co-1-olefins) at the *n*-octane/water interface. Their results show that the interfacial properties depend on the number of carbon atoms in the polyelectrolyte side chain. However, the influence of the kind of hydrocarbon on the *n*-alkane/water interfaces of poly(maleic acid-alt-1-alkene) disodium salts has not been systematically studied. This is the main objective of this work. The experimental results are complemented by theoretical calculations of the energy of interaction between the polyelectrolyte side chains and the kind of hydrocarbon present at the interface.

2. Experimental

2.1. Materials

The polyelectrolytes used were synthesized by mixing a 1:1 mole base, maleic anhydride and the respective 1-alkene (1-octene; 1-decene; 1-dodecene; and 1-tetracene). The radical polymerization was performed using AIBN as initiator (0.3% w:w with respect to monomers) in anhydrous benzene at 55 °C. The reaction time was always 60 min. The polymeric solutions were poured into anhydrous ethyl acetate to obtain white solids, which were dissolved and precipitated twice. Solids were dried under vacuum at room temperature until they attained a constant weight. The molecular weights were estimated by gel permeation chromatography and were in the range of 10,000–12,000. These polymers were characterized by IR spectrophotometry. In order to obtain the respective disodium salts, the above polymers were treated according to the method reported by Chu and Thomas [5]. The resulting polyelectrolytes were characterized by IR and ^{13}C-NMR and were named PC_6, PC_8, PC_{10}, and PC_{12}, respectively, because the two double-bonded carbon atoms primarily belonging to the 1-alkene go into the polymer main chain.

The interfacial tension measurements were performed according to the Du Nöuy method in a Krüss K-8 interfacial tensiometer. All the hydrocarbons were analytical grade from Aldrich, Milwaukee, USA and were treated according to the Lunkenheimer procedure [6] before use. The interfacial tensions between pure phases, γ_{int}^{0}, were 49.2, 50.1, and 50.6 mN/m for the *n*-octane/water, *n*-decane/water, and *n*-dodecane/water interfaces, respectively. All measurements were carried out at 25 ± 0.01 °C. Bidistilled water ultrafiltered through Millipore, with a specific conductivity of 0.2–0.3 μS cm^{-1} was used. All other reagents used were of analytical grade.

2.2. Models and calculation methods

The molecular model used for the calculations were built from the minimal repetition structure but containing two lateral chains, hexyl (C_6), octyl (C_8), decyl (C_{10}), and dodecyl (C_{12}), in the respective interfaces. In these models the terminal methylene groups were replaced by methyl groups. The structures of the polyelectrolyte comonomeric unit (A) and the molecular models (B) derived from those comonomeric units are the following:

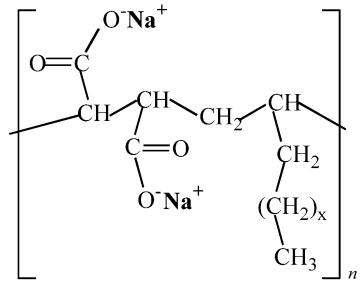

(A)

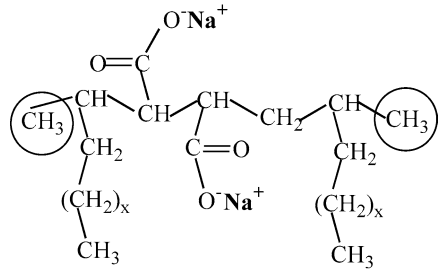

(B)

$x = 4, 6, 8, 10$

Water molecules were not included at the interface due to the complexity that their inclusion implies for the calculations. The latter were done using the Gaussian 98 package [7] at the MP2/6-31G* level. The geometry of each model was fully optimized at that level of the theory. The calculations were performed to determine the interaction energy (ΔE_{int}) between the basic polyelectrolyte models (B) and the respective hydrocarbons, *n*-octane, *n*-decane, and *n*-dodecane at the hydrocarbon/water interfaces, including a counterpoise correction [8]. Such interaction energy is directly related to the experimental standard free energy of adsorption, since the former is a direct measure of the relative stability for the insertion of a hydrocarbon molecule into the space between two lateral chains of the polyelectrolyte.

3. Results and discussion

As an example, Fig. 1 shows the dependence of γ_{int} on the polyelectrolyte concentration, *m*, in mol of comonomeric

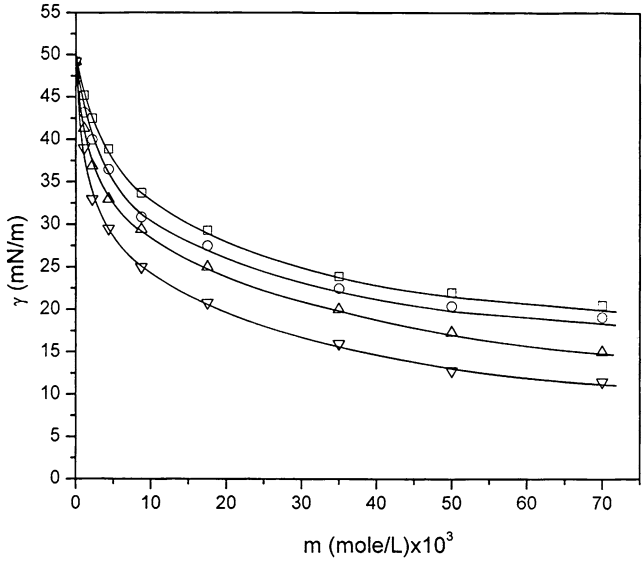

Fig. 1. Interfacial tension dependence on polyelectrolyte concentration at the *n*-octane/water interface: (□) PC_6, (○) PC_8, (△) PC_{10}, (▽) PC_{12}.

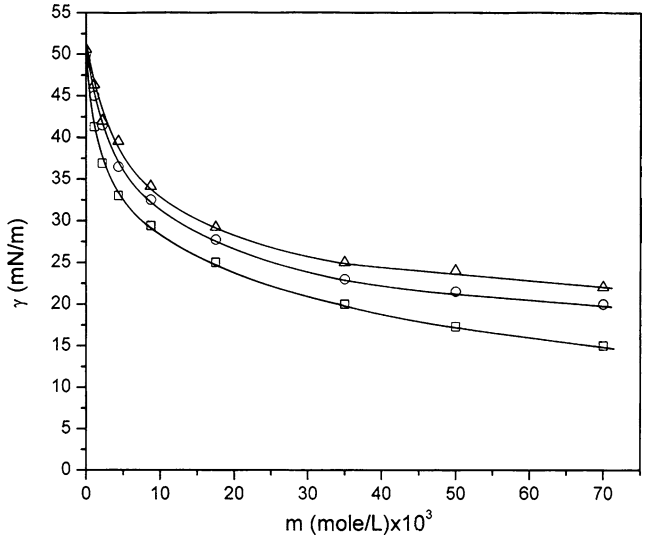

Fig. 2. Interfacial tension dependence on polyelectrolyte concentration for PC_{10}: (□) *n*-octane/water, (○) *n*-decane/water, (△) *n*-dodecane/water.

units/L at the *n*-octane/water interfaces. As can be seen, there is a marked decrease in γ_{int} with m, which is more pronounced as the side-chain length increases. In all the interfaces here studied the same trend was observed. This behavior can be explained in terms of the higher hydrophobic character of the polyelectrolyte as the lateral chain becomes longer, leading to greater interfacial activity. Moreover, the decrease in γ_{int} seems to be more drastic at the *n*-octane/water interface as compared with *n*-decane/water, and *n*-dodecane/water interfaces. For instance, γ_{int} versus m data were plotted as shown in Fig. 2 for the PC_{10} polyelectrolyte. In this plot the kind of polyelectrolyte is constant for the three interfaces here studied. As mentioned above, the decrease is more pronounced at the *n*-octane/water interface. In all the polyelectrolyte systems here studied, similar trends were observed.

In order to quantify and compare the adsorption processes at each interface the Gibbs equation was used [9,10]:

$$\Gamma = -\left[|Z_p Z_g| / \left(|Z_p| + |Z_g|\right)\right] \times RT\,(\mathrm{d}\gamma_{\text{int}}/\mathrm{d}\ln m)(\mathrm{d}\ln m/\mathrm{d}\ln a), \quad (1)$$

where Γ, a, and m are the excess surface concentration, the mean ion activity, and the polyelectrolyte concentration, respectively. Z_p and Z_g are the polyion monomer unit and the counterion valences, respectively, and R and T have their usual meaning. The $(\mathrm{d}\ln m)/(\mathrm{d}\ln a)$ term was evaluated according to Manning's [11] theory by

$$\mathrm{d}\ln a/\mathrm{d}\ln m = \frac{1}{2}\left|Z_g^{-1}\right|(\xi^{-1}) \quad \text{if } \xi > 1, \quad (2)$$

where ξ is the linear charge density parameter, defined as

$$\xi = e^2/\varepsilon kTb. \quad (3)$$

In Eq. (3), e is the proton charge, ε the bulk dielectric constant of the solvent, and b the average distance between charges on the polyelectrolyte chain. The latter value was calculated assuming that C–C–C bond angles and C–C bond distances were 109.5° and 1.54 Å, respectively. Thus, the average values of 6.18 Å, 1.205, and 2.411 were obtained for b, ξ, and $(\mathrm{d}\ln m)/(\mathrm{d}\ln a)$, respectively. Thus, Eq. (2) becomes

$$\Gamma = -[1.205/RT](\mathrm{d}\gamma_{\text{int}}/\mathrm{d}\ln m). \quad (4)$$

Obviously, the surface excess values depend on the charge spacing b and some error may be involved in its estimation. However, this calculated parameter should be very close to the actual distance between charges, considering the high dilution range in which interfacial tension measurements were done. The magnitude of the linear charge density parameter, $\xi = 1.205$, reflects that at the infinite dilution limit, almost 17% of the sodium counterions are condensed onto the polyion to give $\xi = 1$; thus the term $(\mathrm{d}\ln m/\mathrm{d}\ln a)$ in Eq. (2) is not unity, as occurs in single electrolytes. Manning's polyelectrolyte counterion condensation theory [11] reasonably accounts for this fact.

At 25 °C,

$$\Gamma = -[4.86\times10^{-11}](\mathrm{d}\gamma_{\text{int}}/\mathrm{d}\ln m) = -[4.86\times10^{-11}]m(\mathrm{d}\gamma_{\text{int}}/\mathrm{d}m). \quad (5)$$

The slopes, $(\mathrm{d}\gamma_{\text{int}}/\mathrm{d}m)$, were evaluated by fitting the experimental data to the empirical Szyszkowski equation [9],

$$\gamma_{\text{int}} = \gamma_{\text{int}}^0\left\{1 - B\log\left[(m/A)+1\right]\right\}, \quad (6)$$

where γ_{int}^0 is the interfacial tension between pure solvents and A, B are two empirical adjustable parameters. In Table 1 are summarized the values of these parameters for the adjustment of γ_{int} versus m for all the polyelectrolytes and interfaces here studied. The small magnitude of the maximum errors between experimental and theoretical data reflects the appropriateness of the Gibbs–Szyszkowski treatment for accounting for the results in the present case as well. In Figs. 1

Table 1
Adjustment parameters of Gibbs–Szyszkowski equation

Interface	Side chain	$A \times 10^4$	B	Maximum error
n-Octane/water	Hexyl	19.4	0.395	0.67
	Octyl	9.0	0.337	0.44
	Decyl	5.3	0.329	0.20
	Dodecyl	2.5	0.316	0.33
n-Decane/water	Hexyl	26.7	0.397	0.39
	Octyl	15.2	0.351	0.45
	Decyl	8.7	0.326	0.90
	Dodecyl	4.6	0.315	0.99
n-Dodecane/water	Hexyl	40.9	0.399	0.81
	Octyl	21.5	0.365	0.93
	Decyl	12.0	0.336	0.88
	Dodecyl	7.6	0.332	1.08

and 2 the theoretical fitted curves of γ_{int} versus m are also shown.

In Eq. (6), A is a parameter related to the standard free energy of adsorption and B to the average number of molecules per unit area at the interface in its closest packing arrangement or the minimum interfacial area/molecule, i.e., to the limiting excess surface concentration. As can be observed in Table 1, A values increase as the polyelectrolyte side chain length decreases for the same interface, and on the other hand, for the same lateral chain length, these values increase with the hydrocarbon size at the interface. In relation to B values some constancy in their magnitudes is observed with a very slight tendency to decrease as the polyelectrolyte side chain increases. The trend in B values suggests that in this type of systems there is little effect of the lateral chain on the areas covered by comonomer unit at the interface. On the other hand, the A values, being different, suggest unlike standard free energies of adsorption. Moreover, the A, B values are different from those reported by Olea and co-workers [4], which may be mainly attributed to the nature of the counterion, K^+ as compared with Na^+ in the present work, and to the larger polyelectrolyte side chain, 12 to 18 carbon atoms, as compared with 6 to 12 reported in the present work. However, the A values here reported are of the same order of magnitude as those found at the *n*-octane/water interface for monocarboxylate-type polyelectrolytes [1].

In Fig. 3, the Γ dependence on m for the *n*-decane/water interface is shown. These plots were constructed according to Eq. (5). As expected, these curves are Langmuir-type saturation profiles. In all cases, the sequence of the initial slopes $\mathrm{d}\Gamma/\mathrm{d}m$ is the following:

$$(\mathrm{d}\Gamma/\mathrm{d}m)\mathrm{PC}_{12} > (\mathrm{d}\Gamma/\mathrm{d}m)\mathrm{PC}_{10} > (\mathrm{d}\Gamma/\mathrm{d}m)\mathrm{PC}_8 > (\mathrm{d}\Gamma/\mathrm{d}m)\mathrm{PC}_6.$$

Thus, at low m the interface saturation is reached more rapidly with polyelectrolytes containing longer side chains, i.e., chains that cover a larger area at the interface. Moreover, in all cases and for the same interface there was a polyelectrolyte concentration zone where Γ versus m curves

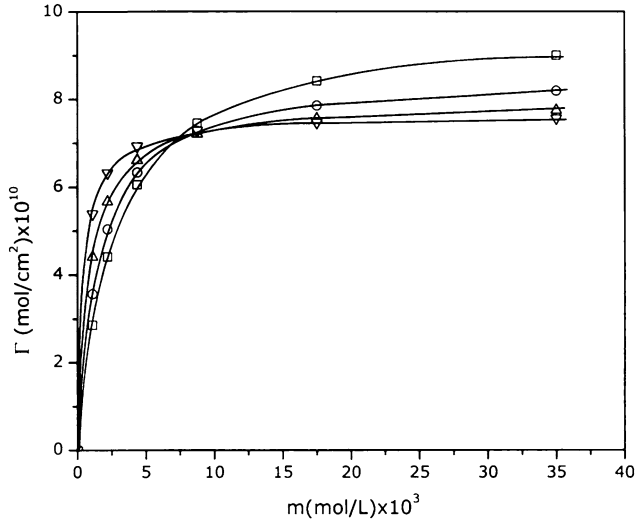

Fig. 3. Excess interfacial concentration at the *n*-decane/water interface: (□) PC_6, (○) PC_8, (△) PC_{10}, (▽) PC_{12}.

intersect each other and beyond this m range the excess interfacial concentration follows the trend

$$\Gamma_{\mathrm{PC}_{12}} < \Gamma_{\mathrm{PC}_{10}} < \Gamma_{\mathrm{PC}_8} < \Gamma_{\mathrm{PC}_6}.$$

In fact, at low m the slopes $\mathrm{d}\Gamma/\mathrm{d}m$ follow the trend mentioned, consistent with the hydrophobic character and the monomer size that these polyelectrolytes have. Thus, PC_6 requires a higher m than PC_{12} to obtain the same Γ due to its less hydrophobic character. On the other hand, at high m, these slopes follow the inverse trend. PC_6 having the shorter side chain is the more hydrophilic polyelectrolyte, and covers at the interface a smaller area than PC_{12}; thus PC_6 requires a higher m than PC_{12} to saturate the interface. Accordingly, in the high m zone, Γ of PC_6 is greater than that of PC_{12} because PC_6 monomer units cover a smaller area than PC_{12}; therefore more PC_6 monomer units can be accommodated at the interfacial region. In the zone where curves intersect each other there is a balance between the hydrophobic character and the size of monomer units covering the available interfacial area. Obviously, PC_8 and PC_{10} are intermediate cases.

By relating Eqs. (5) and (6) it is possible to obtain the following relationship:

$$\Gamma = 4.86 \times 10^{-11}\gamma_{\text{int}}^0\big[Bm/(m + A)\big]. \tag{7}$$

The interfacial saturation condition is reached when $m \gg A$, thus $\Gamma = \Gamma^\infty$, and Eq. (7) becomes

$$\Gamma^\infty = 4.86 \times 10^{-11}\gamma_{\text{int}}^0 B. \tag{8}$$

In Table 2 are summarized the values of Γ^∞ and the areas covered by the comonomeric unit at the interface, σ, calculated as $(N^0\Gamma^\infty)^{-1}$, where N^0 is the Avogadro number. The σ values in Table 2 are practically independent of the nature of the interface for the same polyelectrolyte side chain; however, for the same interface their values increase as the

Table 2
Limiting excess surface concentration, areas covered by comonomer unit, and standard free energies of adsorption

Interface	Side chain	$\Gamma^{\infty} \times 10^{10}$ (mol/cm^2)	$\sigma \times 10^{16}$ (cm^2)	pC_{20}	$-\Delta G^0_{ads}$ (kJ/mol)	$-\Delta E_{int}$ (kJ/mol)
n-Octane/water	Hexyl	9.44	17.57	1.71	21.8	43.73
	Octyl	8.07	20.56	1.84	22.9	46.38
	Decyl	7.88	21.04	2.04	24.2	47.33
	Dodecyl	7.56	21.95	2.30	25.7	49.14
n-Decane/water	Hexyl	9.67	17.15	1.59	21.1	44.96
	Octyl	8.54	19.42	1.70	22.0	49.63
	Decyl	7.93	20.91	1.82	22.9	51.98
	Dodecyl	7.68	21.61	2.07	24.4	54.50
n-Dodecane/water	Hexyl	9.82	16.91	1.45	20.2	46.99
	Octyl	8.98	18.47	1.60	21.3	50.11
	Decyl	8.27	20.06	1.75	22.4	53.25
	Dodecyl	8.15	20.35	1.91	23.3	56.31

lateral side chain increases. Moreover, their values are similar to those reported for esters of saturated acids, long-chain carboxylic acids, and primary alcohols [9,12]. The Γ^{∞} values decrease as the side-chain lengths increase in all cases; however, there is little effect on the interface, with a slight trend to increase as the hydrocarbon size increases. The Γ^{∞} tendency is coherent with the Γ behavior at high polyelectrolyte concentration, as mentioned above.

In all cases, there is a bulk polyelectrolyte concentration where γ_{int} is 20 mN/m units lower than their value at pure interfaces, γ^0_{int}. As Rosen stated [9], at this concentration the interface is 84–99.9% saturated. This concentration, known as C_{20}, is a measure of the adsorption efficiency and pC_{20}, defined as $\log[1/C_{20}]$, a parameter that makes easy to compare the relative adsorption efficiency. Thus the greater the value of pC_{20}, the higher the adsorption efficiency and the lower the bulk polyelectrolyte concentration required to reduce the interfacial tension by 20 mN/m. As can be observed in Table 2 and Fig. 4, for the same polyelectrolyte side-chain length, the pC_{20} values decrease as the hydrocarbon size present at the interface increases. On the other hand, at the same interface, the adsorption efficiency increases as the polyelectrolyte lateral chain increases. These results suggest that polyelectrolytes containing larger side chains are better packed at the interface when the latter contains shorter rather than larger hydrocarbons. In fact, as the polyelectrolyte lateral chain increases, the surface interaction between the hydrocarbon and the polyelectrolyte side chain should increases; thus the higher the molar energy of interaction, the greater the pC_{20}. On the other hand, as the hydrocarbon size increases, the interaction energy per mole between the segments of the polyelectrolyte lateral chain and the hydrocarbon decreases; thus the value of pC_{20} for PC_6 in *n*-dodecane/water interface is just 1.45, the lowest pC_{20} value. At the other extreme, the value of pC_{20} for PC_{12} at the *n*-octane/water interface is 2.30.

In Table 2 are also summarized the values of the standard free energies of adsorption, calculated according to the following equation:

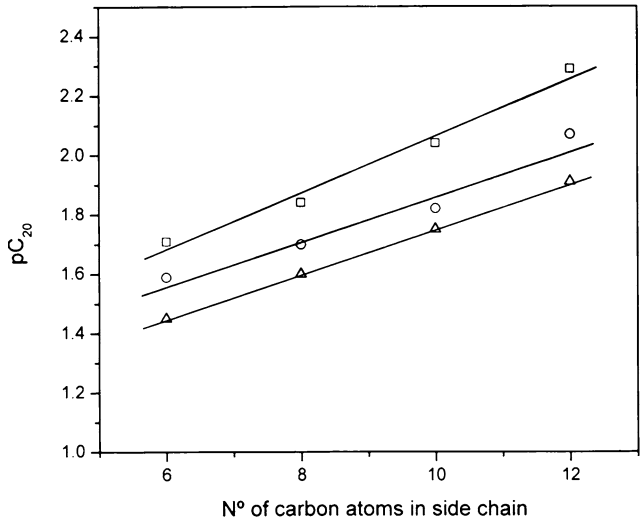

Fig. 4. pC_{20} dependence on number of carbon atoms on the side chain at the (□) *n*-octane/water, (○) *n*-decane/water, and (△) *n*-dodecane/water interface.

$$\Delta G^0_{ads} = -2.303RT[pC_{20} + 1.74] - 120.46\sigma. \quad (9)$$

This equation shows that ΔG^0_{ads} has two negative contributions. The first term is associated with the molar standard free energy of transfer of one comonomeric unit from the bulk to the interface, ΔG^0_{tr}. This term is related to the adsorption efficiency, which is a direct measure of the polyelectrolyte bulk concentration required to induce a determined effect at the interface. The second free energy term, ΔG^0_{int}, is related to the accommodation of the comonomer unit at the interface, i.e., to the minimum surface/molecule ratio at the interface. As stated [9], the latter parameter is a direct measure of the effectiveness of the adsorption process. In Fig. 5, the two free energy terms mentioned above, along with the total ΔG^0_{ads} versus the number of carbon atoms, n_C, in the lateral chain for all polyelectrolytes at the *n*-decane/water interface is shown. This type of plot was linear for all the interfaces here studied and slightly negative reflecting that both free energy processes occur spontaneously. The slopes

Table 3
Slopes of the standard free energies of adsorption

Interface	$-\mathrm{d}(\Delta G^0_{\mathrm{tr}})/\mathrm{d}n_{\mathrm{C}}$ (kJ/mol)	$-\mathrm{d}(\Delta G^0_{\mathrm{int}})/\mathrm{d}n_{\mathrm{C}}$ (kJ/mol)	$-\mathrm{d}(\Delta G^0_{\mathrm{ads}})/\mathrm{d}n_{\mathrm{C}}$ (kJ/mol)
n-Octane/water	0.55	0.09	0.64
n-Decane/water	0.45	0.08	0.53
n-Dodecane/water	0.44	0.07	0.52

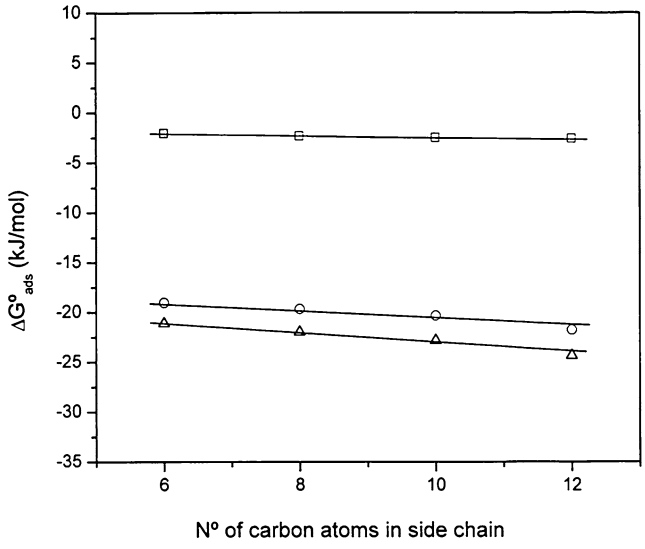

Fig. 5. Adsorption free energies versus number of carbon atoms in the polyelectrolyte lateral chain at the *n*-decane/water interface. (□) $\Delta G^0_{\mathrm{int}}$, (○) ΔG^0_{tr}, (△) $\Delta G^0_{\mathrm{ads}}$.

of these plots, representing the contribution per mole of methylene group to ΔG^0_{tr} and $\Delta G^0_{\mathrm{int}}$, respectively are summarized in Table 3. In all cases the $\mathrm{d}[\Delta G^0_{\mathrm{ads}}]/\mathrm{d}n_{\mathrm{C}}$ values are practically determined by the $\mathrm{d}[\Delta G^0_{\mathrm{tr}}]/\mathrm{d}n_{\mathrm{C}}$ contribution, the $\mathrm{d}[\Delta G^0_{\mathrm{int}}]/\mathrm{d}n_{\mathrm{C}}$ being very small. Thus, the polyelectrolyte adsorption at the hydrocarbon/water interfaces is mainly determined by the contribution of the methylene groups to the adsorption at the hydrocarbon/water interfaces. These $\Delta G^0_{\mathrm{ads}}$ values, ranging from -0.5 to -0.6 kJ/mol, are lower than the -2.55 kJ/mol reported for poly(mono-*n*-alkylmaleic acid-alt-styrene) sodium salts with $n = 8$, 10, and 12 at the *n*-octane/water interface [1]. Differences can be attributed to the nature of the polar head. In fact, in the present case there are two carboxylate groups per comonomer unit, whose electrostatic repulsive interaction acts to desorb the polyelectrolyte from the interface, whereas in the case referred to [1] there is only one carboxylate group per comonomer unit. At the air/water surface, -1.72 kJ/mol has been reported as the contribution to $\Delta G^0_{\mathrm{ads}}$ for the adsorption of each methylene group [13]. On the other hand, the contribution to $\Delta G^0_{\mathrm{ads}}$ per methylene group in poly(4-vinylpyridine) *N*-alkyl quaternized from chloroform to chloroform/water interface is just 0.13 kJ/mol, reflecting that methylene groups act to stabilize this type of polyelectrolyte in the chloroform phase. Therefore, the contribution to $\Delta G^0_{\mathrm{ads}}$ per methylene group depends at least on the following factors: the kind of interface and the solvent where the polyelectrolyte is soluble, the type of polar head of the monomer unit, or, even if it exists, the possibility of a polyelectrolyte intramicellization process in the bulk [5,14]. Olea and co-workers, in a recent paper, reported $\Delta G^0_{\mathrm{ads}}$ data for potassium salts of poly(maleic acid-co-1-olefin) from water to *n*-octane/water interface. We believe that their data have some error, because with the σ and $\mathrm{p}C_{20}$ values reported in Tables 2 and 3, respectively, it is not possible to obtain the $\Delta G^0_{\mathrm{ads}}$ values consigned on the last row of Table 3 and plotted in Fig. 4 of that reference. Table 2 shows that for the same interface the $\Delta G^0_{\mathrm{ads}}$ values decrease, i.e., they become more negative, as the polyelectrolyte side-chain length increases. On the other hand, for the same lateral chain, $\Delta G^0_{\mathrm{ads}}$ values are slightly less negative as the size of the hydrocarbon present at the interface increases. In order to explain this behavior some theoretical calculations were made. The results of the molar energy of interaction, ΔE_{int}, calculated as explained above are also summarized in Table 2. As can be seen, these stabilization energies vary from -43 to -56 kJ/mol for the insertion process of an *n*-octane, *n*-decane, or *n*-dodecane molecule in the cavity formed by two adjacent comonomer hexyl, octyl, decyl, or dodecyl lateral chains. These theoretical results show that the magnitude of the interactions are in the range of the van der Waals-type energies, no matter the length of the polyelectrolyte lateral chains. Furthermore, the distances between the hydrocarbon molecules and these lateral chains are in the range from 2.9 to 3.20 Å, which is also indicative of van der Waals-type interactions. As can be seen in Table 2, the values of the calculated interaction energies are nearly twice the values of the standard free energies of adsorption. This is an interesting result and it can be explained in terms of the nature of the model, which assumes two lateral chains, whereas the $\Delta G^0_{\mathrm{ads}}$ is determined by the monomer unit, which contains only one lateral chain. Thus the models shown in Fig. 6 adequately account for the experimental results in spite of their limitations and they are able to reproduce the experimental trend of the free energy of adsorption within each interface. The theoretical evidence presented shows that the attractions between the model polymer and the hydrocarbon interface are electronic correlation effects, which are essential where there are weak intermolecular attractions. Hence, it is necessary to use at least MP2-level methods for the description of the dispersion forces, including these electronic correlation effects. The theoretical models are not able to describe the change of the interface, due to the fact that their purpose is

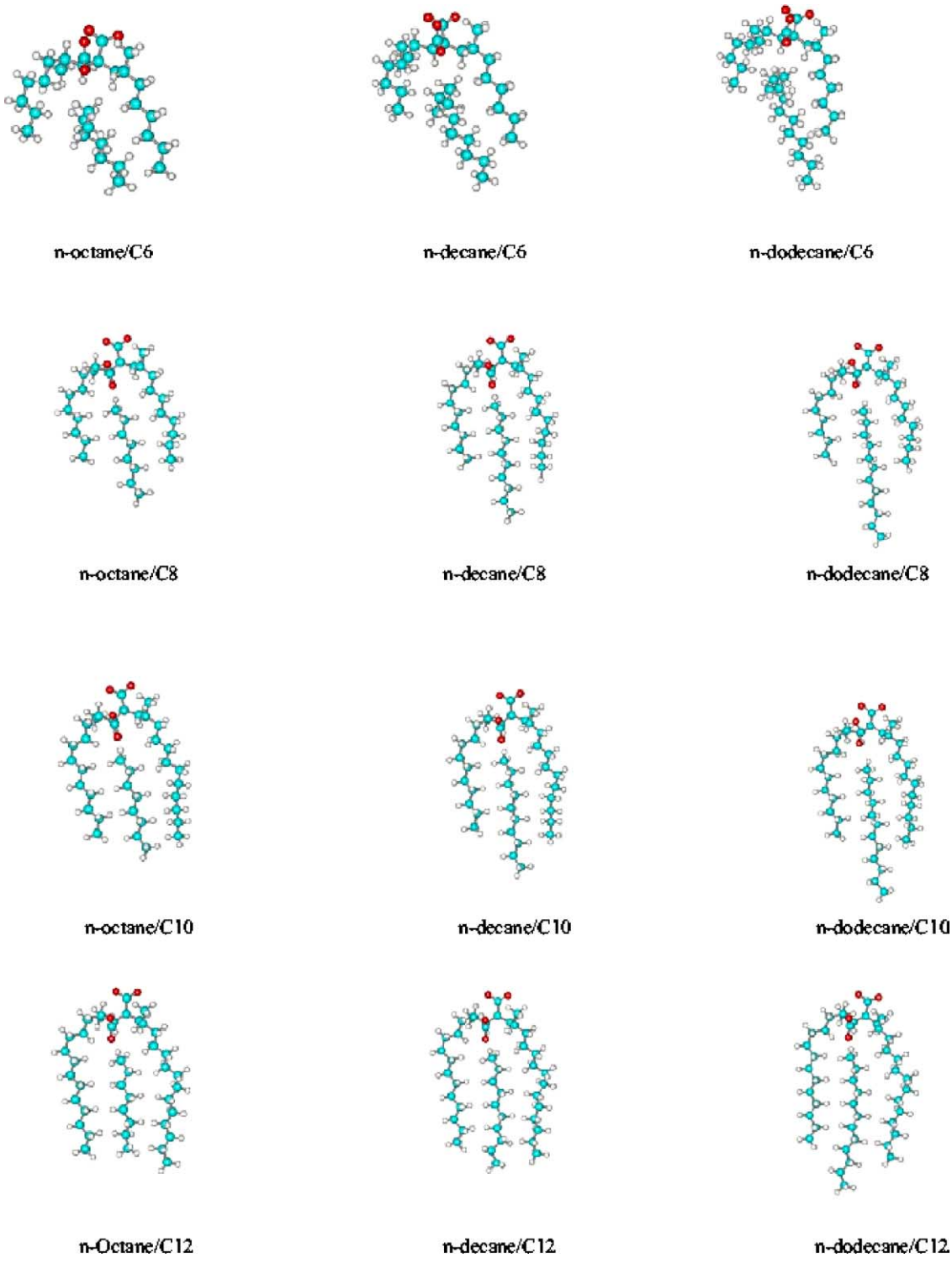

Fig. 6. The interaction models.

to study the nature of the interaction in the space among the lateral chains of each polymer.

On the other hand, Fowkes [15] has pointed out that there is an additional anisotropic dispersion contribution to the interfacial work of adhesion between water and higher *n*-alkanes. This additional contribution becomes relevant for *n*-alkanes higher than *n*-hexane and is roughly proportional to the number of carbon atoms in the alkyl chain above 6. Such an interaction, due to preferential alignment of the longer *n*-alkanes perpendicular to the interface, would appropriately explain the observed results on the bulk-phase dependence of the binding. Such an interaction is not included in our models, since water was not included as a phase. However, for the same *n*-alkane the anisotropic dis-

persion contribution would be approximately constant. Thus, the dispersion term would be very important, as is observed within each experimental and theoretical phase.

The last column of Table 2 shows that the magnitude of the interaction energy increases as the length of the side chain increases vis-à-vis ΔG^0_{ads}. As can be seen in Fig. 6, this trend can be explained in terms of a greater contact surface between the inserted hydrocarbon and the lateral chains as the order of the system increases. Thus, this fact is manifested in greater interaction energies among both fragments, i.e., between the same hydrocarbon molecule and the lateral polyelectrolyte chains. On the other hand, for the same side chain but with increasing size of the hydrocarbon, the contact surface is similar; consequently there are analogous interaction energies, but there exist increasing portions of the hydrocarbon molecules outside of the cavity, which are relatively free to move as compared with the portion inside the cavity. Therefore, this phenomenon results in an increase of the entropy adsorption term, lowering the ΔG^0_{ads}.

From the above results we can conclude that the adsorption process depends on the length of the polyelectrolyte lateral chain. The adsorption process is mainly determined by the adsorption efficiency, i.e., by the standard molar free energy of transfer from water to the interface. Comparatively, the adsorption effectiveness seems to play a much less important role. The molar contribution of the methylene group to ΔG^0_{ads} depends slightly on the nature of the interface. Their values are lower than those reported on micellar systems [16]. This effect may be due to the nature of the polyelectrolyte, where monomer amphipathic units are linked covalently, forming the "polymeric micelle." The small ΔG^0_{ads} values for the methylene group are indicative of van der Waals-type interactions between the hydrocarbon and the side polyelectrolyte chains. Theoretical calculations from a model for the inclusion of hydrocarbon molecules in the cavity formed by two adjacent lateral chains corroborate our observation for the ΔG^0_{ads} trend.

Acknowledgments

The financial support of Fondecyt, Research Grant 1040646, is gratefully acknowledged. The financial aid of the DID (Project I2-03/13-2) and the Department of Chemistry of the Universidad de Chile is also acknowledged. The technical assistance of María Luz Peña is recognized.

References

[1] H.E. Ríos, M.H. Aravena, R.G. Barraza, J. Colloid Interface Sci. 165 (1994) 259.
[2] H.E. Ríos, J.S. Rojas, I.C. Gamboa, R.G. Barraza, J. Colloid Interface Sci. 156 (1993) 388.
[3] M.D. Urzúa, H.E. Ríos, Polym. Int. 52 (2003) 783.
[4] R.G. Barraza, A.F. Olea, F. Martínez, I. Ruiz-Tagle, J. Colloid Interface Sci. 261 (2003) 559.
[5] D.Y. Chu, J.K. Thomas, Macromolecules 20 (1987) 2133.
[6] A. Goebel, K. Lunkenheimer, Langmuir 13 (1997) 369.
[7] M.J. Frisch, G.W. Trucks, H.B. Schlegel, P.M.W. Gill, B.G. Johnson, M.A. Robb, J.R. Cheeseman, K.T. Keith, G.A. Petersson, J.A. Montgomery, K. Raghavachari, M.A. Al-Laham, V.G. Zakrzewski, J.V. Ortiz, J.B. Foresman, J. Cioslowski, B.B. Stefanov, A. Nanayakkara, M. Challacombe, C.Y. Peng, P.Y. Ayala, W. Chen, M.W. Wong, J.L. Andres, E.S. Replogle, R. Gomperts, R.L. Martin, D.J. Fox, J.S. Binkley, D.J. Defrees, J. Baker, J.P. Stewart, M. Head-Gordon, C. Gonzalez, J.A. Pople, Gaussian 98, Rev. A.7, Pittsburgh, PA, 1998.
[8] S.F. Boys, F. Bernardi, Mol. Phys. 19 (1970) 553.
[9] M.J. Rosen, Surfactants and Interfacial Phenomena, Wiley–Interscience, New York, 1989, p. 85.
[10] T. Okubo, J. Colloid Interface Sci. 125 (1988) 387.
[11] G.S. Manning, J. Chem. Phys. 51 (1969) 924.
[12] S. Ross, I.D. Morrison, Colloidal Systems and Interfaces, Wiley, New York, 1988.
[13] J.J. Spitzer, Can. J. Chem. 62 (1984) 2359.
[14] R.G. Barraza, H.E. Ríos, J. Colloid Interface Sci. 209 (1999) 261.
[15] F.M. Fowkes, J. Phys. Chem. 84 (1980) 510.
[16] C. Tanford, The Hydrophobic Effect, Wiley–Interscience, New York, 1988.